

Department of Theoretical and Computational Physics,  
Babeş–Bolyai University



Ph.D. thesis summary

## Statistical Physics Studies of Complex Systems

Szabolcs Endre Horvát

Advisor: Prof. Dr. Zoltán Néda

Cluj-Napoca  
March 2012



# Contents

<b>Contents</b>	<b>i</b>
<b>1 Introduction</b>	<b>1</b>
1.1 Structure of the thesis . . . . .	2
<b>2 Neutral models in ecology</b>	<b>5</b>
A new spatially explicit neutral model . . . . .	6
Empirical data used to test the model . . . . .	7
Relevant macroecological measures . . . . .	8
Relative species abundance distribution (RSA) . . . . .	9
Species-area relationship (SAR) . . . . .	9
The spatial auto-correlation function . . . . .	10
2.1 Simulation results . . . . .	11
<b>3 Entropy production during the final stages of expansion in heavy ion reactions</b>	<b>15</b>
<b>4 Spontaneous synchronization of oscillators</b>	<b>19</b>
The synchronization model . . . . .	22
Modelling and results . . . . .	23
<b>Selected bibliography</b>	<b>27</b>

**Keywords:** complex systems, statistical physics, collective behaviour, neutral theory of biodiversity, voter model, heavy ion collisions, phase transitions, spontaneous synchronization

# Chapter 1

## Introduction

Systems made of a large number of complex parts often show simple patterns in their collective behaviour despite the complexity of the individual parts. The methods of statistical physics are well suited for the study of such phenomena. In recent decades, statistical physics has found applications in an ever increasing number of interdisciplinary fields. It has been applied to problems in such diverse disciplines as ecology, biology, economy, sociology, information science, etc. The systems encountered in these fields are often not easily treated by purely analytical mathematical methods, so the use of computer modelling is necessary. Applying statistical physics methods and modelling in these disciplines has in part been made possible by the cheap availability of powerful computers. Modern technology has also made it possible to collect and store very large datasets which can be used to test theoretical models and to discover new patterns and phenomena.

In this work, three complex systems from three very different disciplines are described. They are studied using Monte Carlo simulations as well as analytical methods. The first part of the thesis describes a spatially explicit model, based on the neutral theory of biodiversity, that can reproduce the spatial distribution of tree species in tropical forests. In particular, the model introduced can reproduce with great accuracy the number of different species that can be found on a given area. In the second part, basic thermodynamic considerations are used to draw conclusions about the final

expansion stage of the quark gluon plasma created in an ultra-relativistic collision of heavy atomic nuclei. The method is applied to interpret the output of a relativistic fluid dynamical simulations describing the expansion. The third part describes several variations on a simple synchronization model of bimodal oscillators with a pulse-like coupling. The phase space of the oscillator system is explored in great detail, revealing an unexpectedly complex structure. It is shown that the system is capable of spontaneous synchronization under more general conditions than previously thought.

## 1.1 Structure of the thesis

The thesis is structured into three parts, each of which describes a different kind of complex system. Methods of statistical physics and Monte Carlo simulations are used to study each of them. The results have been published in four papers and accepted at a conference (see references [4], [3], [5], [6] and [7]). My contributions to each one are described below.

1. The first part describes a spatially explicit version of the neutral theory of ecology. The neutral theory of ecology was created to explain the distribution of similar biological species according to their abundance. There have been efforts to extend this theory to describe the distribution of species in space as well. We have developed a spatially explicit version of the neutral model of ecology which can successfully reproduce certain characteristics of the spatial distribution of tree species in tropical forests. In particular, our model can reproduce precisely the species-area curve, i.e. the number of different species found in an area of a given size. The findings have been published in the following paper:

Sz. Horvát, A. Derzsi, Z. Nédá, and A. Balog, *A spatially explicit model for tropical tree diversity patterns*, **Journal of Theoretical Biology**, vol. **265**, no. 4, pp. 517-523, 2010.

My main contribution to this paper was developing the software to simulate the spatially explicit model, running the simulations and

fitting the parameters to the empirical data, then finally analysing the results.

2. The second part describes a simple thermodynamic approach to studying the final stages of the expansion of the quark gluon plasma created in a high energy collision of heavy nuclei.

Sz. Horvát, V. Magas, D. Strottman, and L. Csernai, *Entropy development in ideal relativistic fluid dynamics with the Bag Model equation of state*, **Physics Letters B**, vol. **692**, no. 4, pp. 277-280, 2010.

I developed a method to correctly calculate thermodynamic variables during the final stages of expansion in a fluid dynamical model of heavy-ion collisions, when the pressure approaches zero, and applied the method to interpret the output of a relativistic fluid dynamical simulation, considering the effects of numerical viscosity. I performed all the necessary analytical and numerical calculations.

3. The third part of the thesis describes a system of bimodal stochastic oscillators with pulse-like coupling. The oscillators are coupled through an interaction that does not include explicitly phase-difference minimizing forces. Instead, the coupling between the oscillators aims to minimize the difference between the output level of the system and a threshold level. As a side effect of this optimization interaction, the oscillators become synchronized. Several models of this type have been studied using numerical modelling, and a phase space with a remarkably complex structure has been uncovered while exploring the behaviour of the oscillator ensemble as a function of the ratio of the periods of the modes and the threshold parameter.

Sz. Horvát, E. Á. Horváth, G. Máté, E. Káptalan, Z. Néda, *Unexpected synchronization*, **Journal of Physics: Conference Series**, vol. **182**, 012026, 2009

Sz. Horvát, Z. Néda, *Complex phase space of a simple synchronization model*, manuscript submitted to the New Journal of Physics, <http://arxiv.org/abs/1203.1699>

My main contributions are developing software that can simulate the system of oscillators significantly faster than previous methods, and the development of an adaptive sampling method that allows mapping the phase space of the system with high precision while needing to run the simulation only for relatively few points in the phase space. I used numerical modelling to study the system as a function of the ratio of the periods of the oscillation modes and the threshold parameter.

# Chapter 2

## Neutral models in ecology

Ecology is the science that studies interactions between various living organisms, as well as these organisms and their environment. Living organisms are highly complex, thus, in practice it is not possible to describe and model their relationships in a completely general and precise mathematical way. Despite this, in certain cases some strikingly simple patterns can be observed in data collected about ecological systems, which hint at the existence of relatively simple dominant mechanisms that are responsible for shaping them. Mathematical ecology aims to discover and model these mechanisms using the tools of mathematics.

The neutral theory of biodiversity was developed to better understand the abundance distribution of species. Why are there so many different species in tropical forests? How can they all coexist in the same environment? Why are some species more common than others? The classical answer of ecology to this question is that all species differ in some important ways from all others, thus they can share the available range of resources by specialization and avoiding strong competition.

The classical viewpoint of ecology is based on the concept of ecological niches. *Niche* means the collection of all factors that influence the survival of a particular species. This includes all resources a species consumes, such as food sources, its habitat, its hunting grounds and breeding grounds, its predators and parasites, etc. Does a herbivore eat grass or leaves? Does

a bird nest on the ground or in the canopy? All these factors differentiate species from each other and reduce the surface of competition between them. In this way each species has its own “ecological compartment” or *niche*, which it occupies alone, without needing to compete for each resource with another species. According to the principle of competitive exclusion, no two species can share the same ecological niche. It is held that if two species consume the exact same resources under constant environmental conditions, then one of them will always be better adapted to these conditions than the other, and will displace the other one.

In the recent two decades a new viewpoint has emerged which starts from the assumption that all similar species can be considered equivalent to each other. The idea was set forth in a now classical work by Stephen Hubbell [8]. Theories built on this assumption are called neutral theories. These have caused some controversy because their fundamental assumption contradicts the principle of competitive exclusion [14]. Despite the obvious oversimplification they make, stochastic models built on the neutral theory have managed to reproduce the distribution of similar species according to their abundances quite well [19, 18, 1]. This suggests that at least in the case of similar species, stochastic processes play an important role in determining species abundances.

## A new spatially explicit neutral model

The original version of the neutral model of biodiversity [8] easily lends itself to a spatially explicit extension where each of the individuals has an assigned spatial position [14, 20]. This is a particularly appropriate description when considering species that do not move around, such as trees in a forest. For simplicity, from now on we shall refer to individuals as “trees”.

Zillio et al. have described such a spatially explicit version of Hubbell’s neutral model, based on the voter model [20]. Following in Zillio’s footsteps, we extended Hubbell’s original model to include the spatial positions of individuals (in this case: trees). The most straightforward way to do this is to consider a lattice model: each site of a square lattice is occupied by a tree.

Like in Hubbell's original model, each individual has the same probability of dying, regardless of species or age. The rules describing the time evolution of the system are the following:

In each discrete time step, randomly choose a lattice site.

1. With probability  $1 - q - p$ , the state of the chosen site is changed to one of its 8 Moore-neighbours. This is the most probable outcome, and models the quite common case of the new individual being an offspring of a neighbouring tree.
2. With probability  $q$ , a randomly selected species is assigned to the chosen site. This species is selected with a uniform probability from the ensemble of possible species. If the potential number of species from which the selection is made is big enough and  $q$  is much smaller than one, this process is suitable for modelling speciation or immigration into the considered territory.
3. With probability  $p$ , the species identity of the new tree is chosen to be the same as the species of a randomly selected individual from among the remaining  $N - 1$  ones. This rule models the diffusion of the seeds in the considered area, allowing seeds originating from faraway individuals to reach the location.

Although this is a relatively simple, two-parameter model, handling it analytically has proven difficult. Therefore it was studied using Monte Carlo simulations on a computer.

## Empirical data used to test the model

The experimental results used for testing the model are from a detailed 50 hectare tropical forest tree census in Barro Colorado Island (BCI), realized by the Smithsonian Tropical Research Institute, Center for Tropical Forest Science (CTFS) [2]. BCI is located in the Atlantic watershed of the Gatun Lake (Panama) and was declared a biological reserve in 1923. It has been administrated by the Smithsonian Tropical Research Institute since 1946.

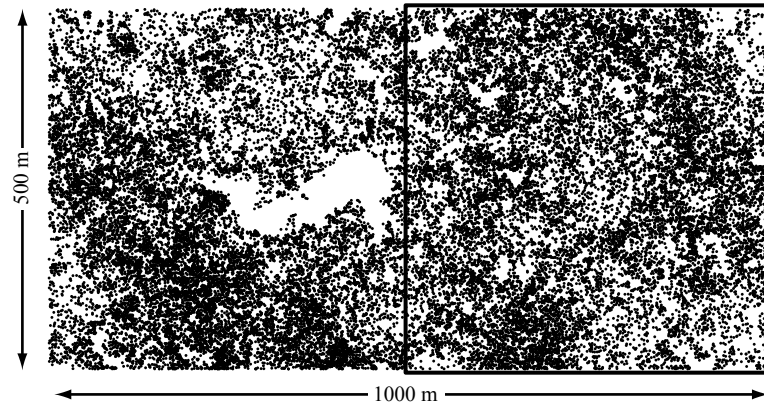


Figure 2.1: The spatial distribution of the most abundant species, *Hybanthus prunifolius*, in the Barro Colorado Island tree census, census year 1995. The square on the right shows the area that was used for calculating statistic.

From the viewpoint of ecological studies, this island is ideal because it is covered with a rainforest that is still undisturbed by humans. The flora and fauna of BCI have been studied extensively and inventories have reported 1369 plant species, 93 mammal species (including bats), 366 avian species (including migratory), and 90 species of amphibians and reptiles. The tropical tree census was performed only on a small part of the island, precisely on a  $1000 \times 500$  metre (50 hectare) area. The first census was completed in 1982, revealing a total of approximately 240,000 stems of 303 species of trees and shrubs. The importance of this CTFS programme consists in the fact that in each census all free-standing woody stems at least 1 cm diameter at breast height are identified, tagged, and mapped, and hence accurate statistics can be made. Data is publicly available for the years 1982, 1985, 1990 and 1995 [2].

### Relevant macroecological measures

Three quantitative measures were used to compare the simulation results to the empirical data. They are briefly described in the following.

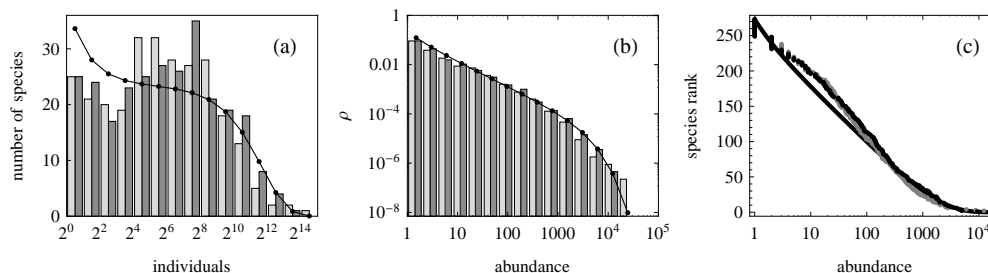


Figure 2.2: Simulation results (dark grey) for the relative species abundance curve after 50,000 Monte Carlo steps, compared with the measurement data (light grey), and the predictions of the Fisher log series for  $\alpha = 33.64$  (solid black lines). Panel (a) shows the Preston plot, (b) the probability density function, and (c) the rank-abundance plot. Simulation parameters:  $L = 500$ ,  $p = 0.3$  and  $q = 1.3 \times 10^{-4}$ .

### Relative species abundance distribution (RSA)

There are three simple ways of representing the relative abundance of species. The first and most widespread is called a Preston-plot and is simply an illustration of how many species are there that have 1, between 2 and 4, 4 and 8, 8 and 16, etc. individuals in the considered experimental sample.

It is mathematically more rigorous to work with an actual probability distribution. This can be represented as either as a probability density function or a cumulative distribution function. These have been used as well.

### Species-area relationship (SAR)

The species area relationship is the function  $S(A)$  that gives the mean number of species,  $S$ , that can be found on an area of size  $A$ . In the past it has been conjectured that  $S(A)$  often follows a power law, therefore a logarithmic scale was used to show it (and highlight the differences from a power law behaviour).

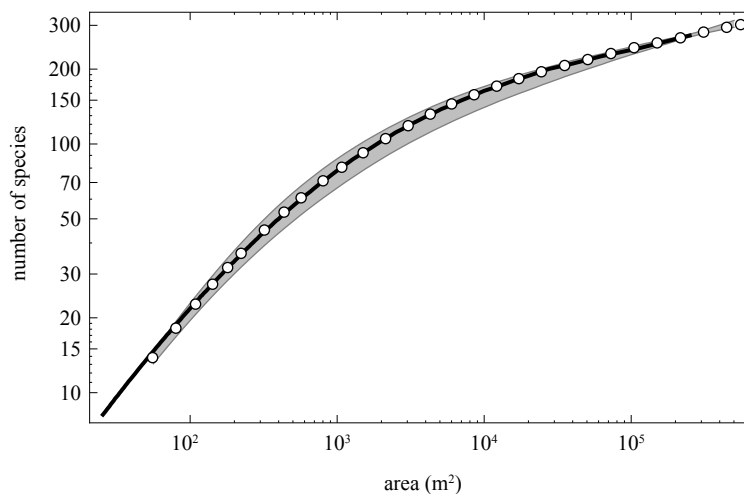


Figure 2.3: Species-area curves: comparison of simulation (grey shaded area) and experimental (black line) results. The shaded area was computed from a set of 50 simulation runs, and represents the mean value  $\pm 2$  standard deviations. The white circles represent one simulation result that fits the experimental data best. Simulation parameters:  $L = 500$ ,  $p = 0.3$  and  $q = 1.3 \times 10^{-4}$ . Experimental data: BCI 1995.

### The spatial auto-correlation function

The final quantitative measure used for testing the model is the spatial auto-correlation functions of the density of common species.

Let  $N_{i,j}$  denote the number of individuals belonging to a given species that can be found in cell  $(i, j)$  of a square grid. Then the auto-correlation function associated with the distribution of this species is defined as

$$C_{p,q} = \langle (N_{i,j} - \langle N \rangle)(N_{i+p,j+q} - \langle N \rangle) \rangle_{i,j} \quad (2.1)$$

$\langle N \rangle$  denotes an average over all cells. It is reasonable to assume that the density of individuals is isotropic, so it is advantageous to use the azimuthally averaged auto-correlation function:

$$C(r) = \langle C_{p,q} \{ r \leq \sqrt{p^2 + q^2} \leq r + \Delta r \} \rangle_{p,q} \quad (2.2)$$

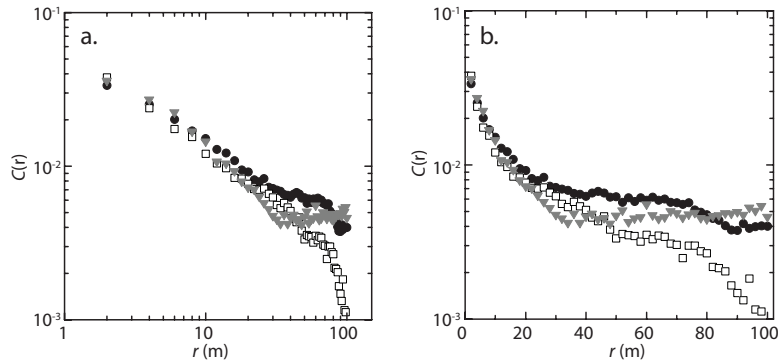


Figure 2.4: The  $C(r)$  spatial auto-correlation function for the three most abundant species of the BCI census: *Hybanthus prunifolius* (white squares), *Faramaea occidentalis* (black circles), and *Trichilia tuberculata* (grey triangles). Census year: 1995. The same function is plotted on a log-log scale on panel (a) and a linear-log scale on panel (b).

The spatial auto-correlation function of the most abundant species in the BCI dataset was found to decay as a power law function, as shown in figure 2.4.

## 2.1 Simulation results

The model was studied using Monte Carlo type simulations.

When the parameter  $p$  is set to 0, our model becomes equivalent to Zillio's. However, in this case individuals belonging to the same species will cluster together in a way that is clearly unrealistic. Thus a  $p > 0$  parameter value was used.

The model parameters  $p$  and  $q$  were optimized to reproduce two quantities from the BCI dataset: (1) the number of species present on a 25 ha area; (2) the slope of the log-log SAR curve in the neighbourhood of the 25 ha area. By optimizing for these two quantities only, the RSA, as well as the SAR for the whole range of available area values could be reproduced.

An extensive search of the parameter space using numerical modelling

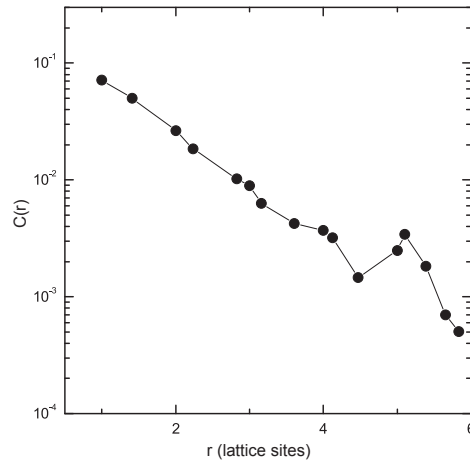


Figure 2.5: The auto-correlation function of the most abundant species obtained from the simulation after 50000 Monte Carlo steps. Note that the scale for  $C(r)$  is logarithmic, while the scale for the radius is linear. Simulation parameters:  $L = 500$ ,  $p = 0.3$  and  $q = 1.3 \times 10^{-4}$ .

gave the parameter values  $p = 0.3$  and  $q = 1.3 \times 10^{-4}$ , which resulted in the best fit to the empirical data. As expected, the spatial model can reproduce the relative species abundance curves observed in nature very well. These are shown in figure 2.2.

The optimal parameter values were then used to run a new set of simulations for the purpose of comparing the species-area relationship for the full range of area values. The results are shown in figure 2.3. The black curves represents the SAR computed from the Barro Colorado Island census data while the grey shaded area shows 50 simulation results, and represents their mean value  $\pm 2$  standard deviations. The white circles represent the model result that matches the empirical SAR best.

Even though the model parameters were optimized by fitting only two numbers (the total number of species found on a given area and the derivative of the SAR curve at this point), the empirical SAR is reproduced by the model very accurately. This is a significant result because it shows that the model can be practically used to predict the number of species that can

be found on a given area, based on measurements at a different area scale.

Unfortunately this model was not able to reproduce the spatial auto-correlation function well. The auto-correlation function of the abundant species decays exponentially in simulation results, as shown in figure 2.5. This contradicts the power-law decay observed in nature and shown in figure 2.4.



## Chapter 3

# Entropy production during the final stages of expansion in heavy ion reactions

In high energy collisions of heavy atomic nuclei, a new state of matter can be created, the Quark-Gluon Plasma. This is a remarkable state of matter because the quarks are able to move freely within it.

The Quark-Gluon Plasma was shown to behave like a low viscosity fluid in experiments, therefore fluid dynamical approaches are suitable for studying it. Except for the most trivial configurations, the equations of relativistic fluid dynamics can only be solved numerically, on a computer. However, numerical methods can only give an approximate solution to equations. The difference between the (unknown) analytic solution and the numerical solution is called the numerical error. Part of the numerical error in fluid dynamical computations arises in the form of numerical viscosity. That is, even when solving the equations of a perfect fluid, some viscosity will be present in the solution due to the effect of the finite resolution of the computational grid.

It is important to note that the equations of perfect fluid dynamics are unstable. In real fluids, some viscosity is always present, therefore large instabilities do not always arise. Therefore it is not our goal to find the

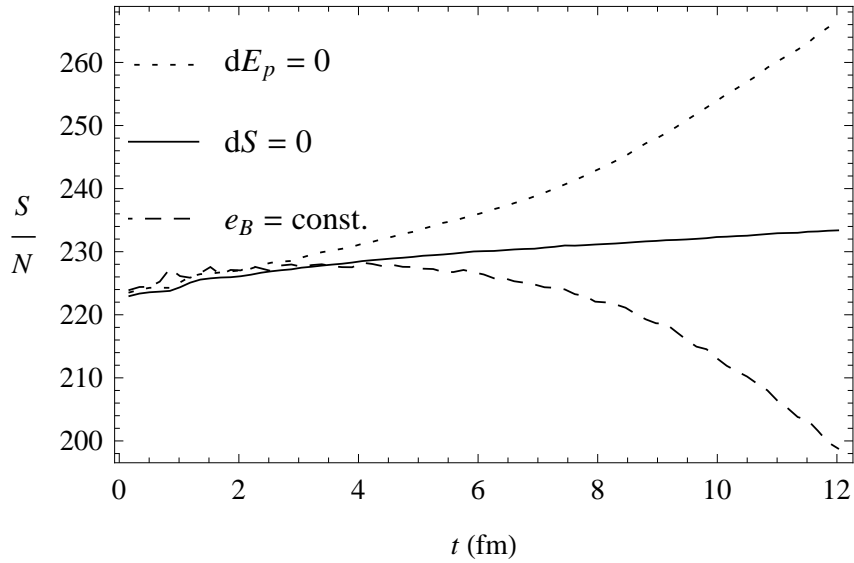


Figure 3.1: Change of the mean specific entropy  $S/N$  in time during expansion in a numerical fluid dynamic computation. The dashed line corresponds to the assumption that the Bag energy density is constant. This leads to decreasing entropy, which conflicts with the second law of thermodynamics. The solid line represents an adiabatic expansion of the quark gas component. The slight entropy increase here (of 5-6%) is due to the numerical viscosity of the computational method. The dotted line corresponds to the assumption that the total energy of the gas component is constant during expansion. The cell size was  $dx = dy = dz = 0.575$  fm

exact solution of the equations of non-viscous fluid dynamics. Instead, the numerical viscosity arising from the discretization of these equations is set equal to the (slight) physical viscosity.

The numerical fluid dynamics code that we use is based on the Particle in Cell method and is highly stable. It can run stably up to the final stages of expansion where the pressure becomes zero. Our approach is to let the fluid dynamical model run beyond the point of freeze-out. The freeze-out hypersurface can then be determined from external parameters that are not used in to solve the fluid dynamical model. The temperature and density

can provide guidelines.

To be able to solve the equations of fluid dynamics, it is necessary to complement them with an equation of state that connects the pressure, baryonic density and energy density. Note, however, that quantities such as temperature and entropy do not appear in the calculation. These can be determined from the baryonic density and energy density after the code has run. In our code, we used the simple Bag model equation of state. This equation of state yields negative pressures for low energy densities, which would indicate an (unphysical) tendency for clusterization. To avoid this, the pressure was set to zero at low energy densities. Then the entropy and temperature must be calculated in accordance with this change.

The Bag model assumes that a gas of partons is moving in a background field of constant energy density. When calculating the entropy and temperature in the energy density regions where the total pressure is zero, it is necessary to consider the exact nature of energy exchange between the parton gas and the background field. We used thermodynamic methods to consider three cases, each of which results in a different entropy evolution of the system.

It was found that in order for the entropy not to decrease (and to satisfy the second law of thermodynamics), it is necessary that the energy density of the background field decreases during expansion. The interaction measure was calculated as well, and compared to curves obtained from Lattice QCD calculations.

The method developed was applied to interpreting the output of a fluid dynamical simulation. The results for the change in entropy are shown in figures 3.1.

It is conjectured that the hadronization and freeze-out may proceed through a Quarkyonic phase, where the chiral symmetry is broken and the quarks gain mass. This corresponds to the gradual disappearance of the background field in these calculations.



# Chapter 4

## Spontaneous synchronization of oscillators

Synchronization means the adjustment of the rhythm of periodic oscillators by means of a weak interaction between them, so that they begin operating at the same frequency.

Spontaneous synchronization appears in a wide variety of systems in nature. Well-known examples include biological systems such as fireflies flashing in unison or crickets chirping together [15], rhythmic applause [10, 11], pacemaker cells in the heart [13], the menstrual cycles of women living together [16], oscillating chemical reactions, mechanically coupled metronomes, pendulum clocks hung on the same wall, and many other systems.

Several models exist that aim to describe spontaneous synchronization. These can be grouped into two broad categories: those that have a phase-minimizing coupling between individual oscillators and those that have a pulse-like coupling. The basic example of a phase-coupled system is the Kuramoto model, while a simple example of a pulse-coupled oscillator model is the integrate-and-fire model. Both of these model types have a parameter characterizing the tightness of coupling between the oscillating units. When global coupling is present, a phase transition is possible in these models: they demonstrate a sudden appearance of partial synchronization when the

coupling parameter is increased above a threshold level.

Recently a new synchronization model has been described. It consists of stochastic bimodal oscillators with a pulse-like coupling. At any time, each oscillator can be active, emitting a signal, or inactive. The sum of the emitted signals gives the total output level of the system. This synchronization model is remarkable in that unlike previous models, it does not contain any explicitly phase difference minimizing interactions. Instead, the dynamic of the units strives to minimize the difference between the total output of the system and a threshold level. Each oscillator can operate in a fast or slow mode, “flashing” quickly or slowly. The periods of the two modes are not constant, but random variables. The average output intensity of the units is different in the two modes. At the beginning of each period, an oscillator will choose which mode to follow depending on the total output level in the system. If the total output is greater than a threshold, it will choose the slow mode so as to decrease the total average output. If the total output is less than a threshold, it will choose the fast mode to increase the output. Interestingly, this optimization dynamic leads to the emergence of partial synchronization in the system. When the system reaches a steady state, the oscillators will flash in union [12, 9].

Several variations on this model are possible, depending on the duration of the active and inactive phases in the two modes [12, 4, 17, 6]. We have studied three different models using numerical simulations, as a function of the threshold level [4, 6], the parameter characterizing the randomness of the periods and the ratio of the periods of the two modes. A fast numerical simulation code was developed in conjunction with an adaptive sampling method to map the structure of the phase space of the model. When studying the models as a function of the ratio of the oscillation mode periods, a complex phase space has been uncovered with many phases (figure 4.1, in each of which the total output level of the system has a different shape (see figure 4.3). It was shown that partial synchronization can emerge under very general conditions, and synchronization is possible even when the coupling does aims to maximize (not minimize) the difference between the total output and the threshold level.

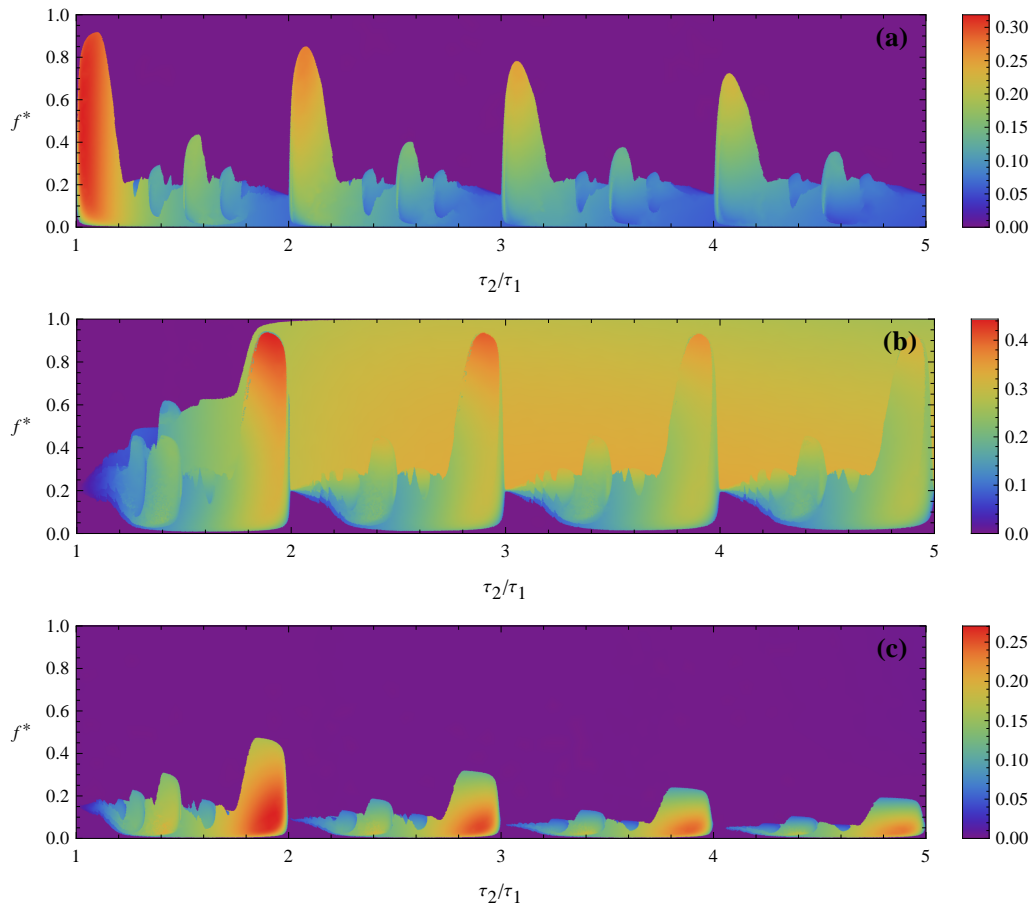


Figure 4.1: The order parameter  $\sigma$  shown as a function of the parameters  $\tau_2/\tau_1$  and  $f^*$ , for the three different models. **(a)** Model 1: the duration of the lit phase (C) is fixed while the duration of the dark phase (B) is variable. Simulation parameters:  $N = 10000$ ,  $\tau_C = 0.15$ . **(b)** Model 2: the duration of the dark phase (B) is fixed while the duration of the lit phase (C) is variable. Simulation parameters:  $N = 10000$ ,  $\tau_B = 0.8$ . **(c)** Model 3: the duration of the dark phase (B) is variable and the duration of the lit phase is fixed, like in the case of model 1, however the interaction strived to maximize the difference between the total output level and  $f^*$ . Simulation parameters:  $N = 10000$ ,  $\tau_C = 0.15$ .

## The synchronization model

The basic version of the model considers an ensemble of  $N$  identical bimodal, globally coupled, stochastic oscillators. At any time, an oscillator can either be active, emitting a signal of strength  $1/N$ , or inactive, emitting no signal. Therefore the total output level of the system can vary between 0 and 1. These oscillators can be intuitively thought of as flashing units. For simplicity, from now on we shall refer to active ones as *lit* and inactive ones as being in an *unlit* or *dark* state. In accordance with this intuitive picture, the sum of the units' output levels can be thought of as the total light intensity in the system.

The units are stochastic bimodal oscillators. They can operate in two oscillation modes, one with a shorter and one with a longer period. These will be referred to as mode 1 and mode 2, respectively. The periods of the modes are random, and their mean values are denoted by  $\tau_1$  and  $\tau_2$ .

An oscillation period consists of three phases,  $A$ ,  $B$  and  $C$ . During phase  $A$  and  $B$  the units are dark, while during phase  $C$  they are lit. The duration of phase  $A$ ,  $\tau_A$ , is an exponentially distributed random variable with mean  $\langle \tau_A \rangle = \tau^*$ . The duration of phase  $B$ ,  $\tau_B$ , can have two values,  $\tau_{B1}$  and  $\tau_{B2}$ , corresponding to the two oscillation modes. The duration of the lit phase,  $\tau_C$ , is fixed. The average lengths of the periods of the modes is the sum of the mean durations of these three phases:  $\tau_1 = \langle \tau_A \rangle + \langle \tau_{B1} \rangle + \langle \tau_C \rangle = \tau^* + \tau_{B1} + \tau_C$  and similarly  $\tau_2 = \tau^* + \tau_{B2} + \tau_C$ . Since the units stay lit for a greater fraction of the short period mode than the long one, the average light intensity will be larger when the units are oscillating in the short period mode.

The coupling between the oscillators is realized through an interaction that strives to optimize the total light intensity in the system, denoted  $f$ . At the beginning of each period, a unit decides which mode to follow based on whether the total light intensity,  $f$ , is greater or smaller than a threshold level  $f^*$ :

- If  $f \leq f^*$ , the shorter period mode will be chosen. Since an oscillating unit stays lit for a greater fraction of a full period when it is operating in the short mode, this will help in increasing the average

light intensity in the system.

- If  $f > f^*$ , the longer period mode will be chosen, reducing the average total light intensity in the system.

According to these rules, each oscillating unit individually aims to achieve a total output intensity as close to  $f^*$  as possible, based on their instantaneous measurements of the output level. As a side effect of this optimization procedure, synchronization can emerge: the total output intensity of the system becomes a periodic function and the units will flash in unison.

## Modelling and results

In this work we have focused on three variations of the basic model described above: **model 1.** the basic model described above with a fixed-duration lit phase, and a variable duration dark phase; **model 2.** a model with variable duration lit phase and a fixed-duration dark phase; and **model 3.** fixed-duration lit phase and variable duration dark phase with a reversed choice of the long or short modes depending on the  $f^*$  value. This last case will be referred to as “anti-optimization” because the oscillators strive to achieve an output as different from  $f^*$  as possible. Partial synchronization emerges in all three cases.

To detect partial synchronization in the system, i.e. a global output intensity function  $f(t)$  that corresponds to “flashing”, the standard deviation of the total output function,  $\sigma$ , was used:

$$\sigma = \lim_{x \rightarrow \infty} \sqrt{\frac{1}{x} \int_0^x (f(x) - \langle f(x) \rangle)^2 dx}$$

where

$$\langle f(x) \rangle = \lim_{x \rightarrow \infty} \frac{1}{x} \int_0^x f(x) dx.$$

A large standard deviation indicated a large variation in the output intensity.

The behaviour of the models was explored as a function of the ratio of the periods of the average oscillation modes,  $\tau_2/\tau_1$  and the threshold parameter

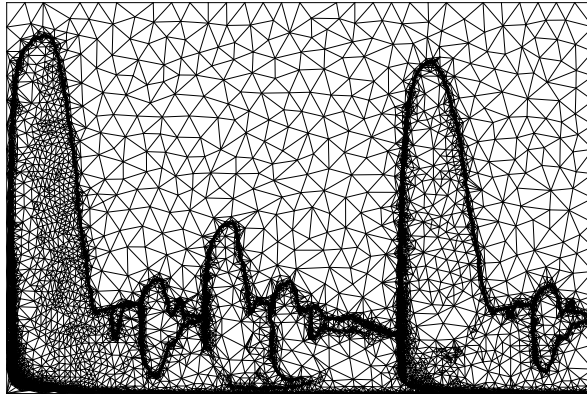


Figure 4.2: The sampling mesh used to compute part of figure 4.1a. Note that most points are clustered around the discontinuities. An irregular triangular mesh was used as starting point, and then iteratively refined.

$f^*$ . Mapping the phase precisely space takes a huge computation effort, so an adaptive sampling method was developed to reduce computation efforts. The method made it possible to use more sampling points around parameter values where the behaviour of the system changed quickly, while using only a few points in regions where a change of parameters does not induce a significant change in behaviour. An example point mesh generated by this adaptive sampling method is illustrated in figure 4.2.

We found that the phase space of this system has a strikingly complex structure with several phases separated by a discontinuous jump in the order parameter  $\sigma$ . In each of these phases, the shape of the total output intensity function of the ensemble,  $f(t)$ , is different.

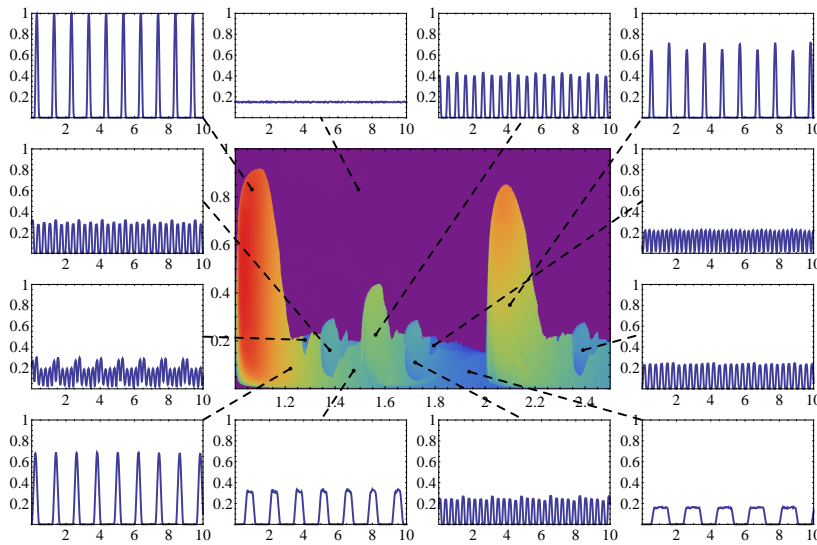


Figure 4.3: The shape of the output signal for model 1 for various parameter values. The simulation parameters were  $N = 10000$  oscillators and  $\tau_C = 0.15$ .

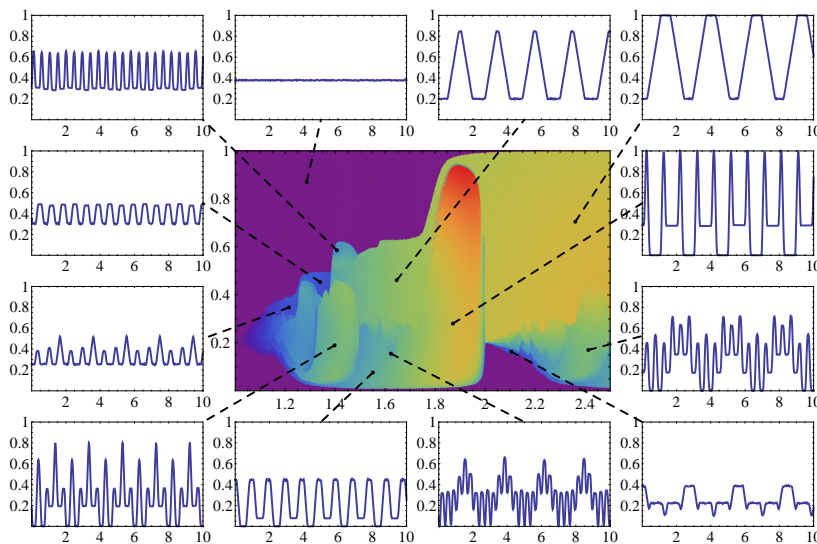


Figure 4.4: The shape of the output signal for model 2 for various parameter values. The simulation parameters were  $N = 10000$  oscillators and  $\tau_B = 0.80$ .

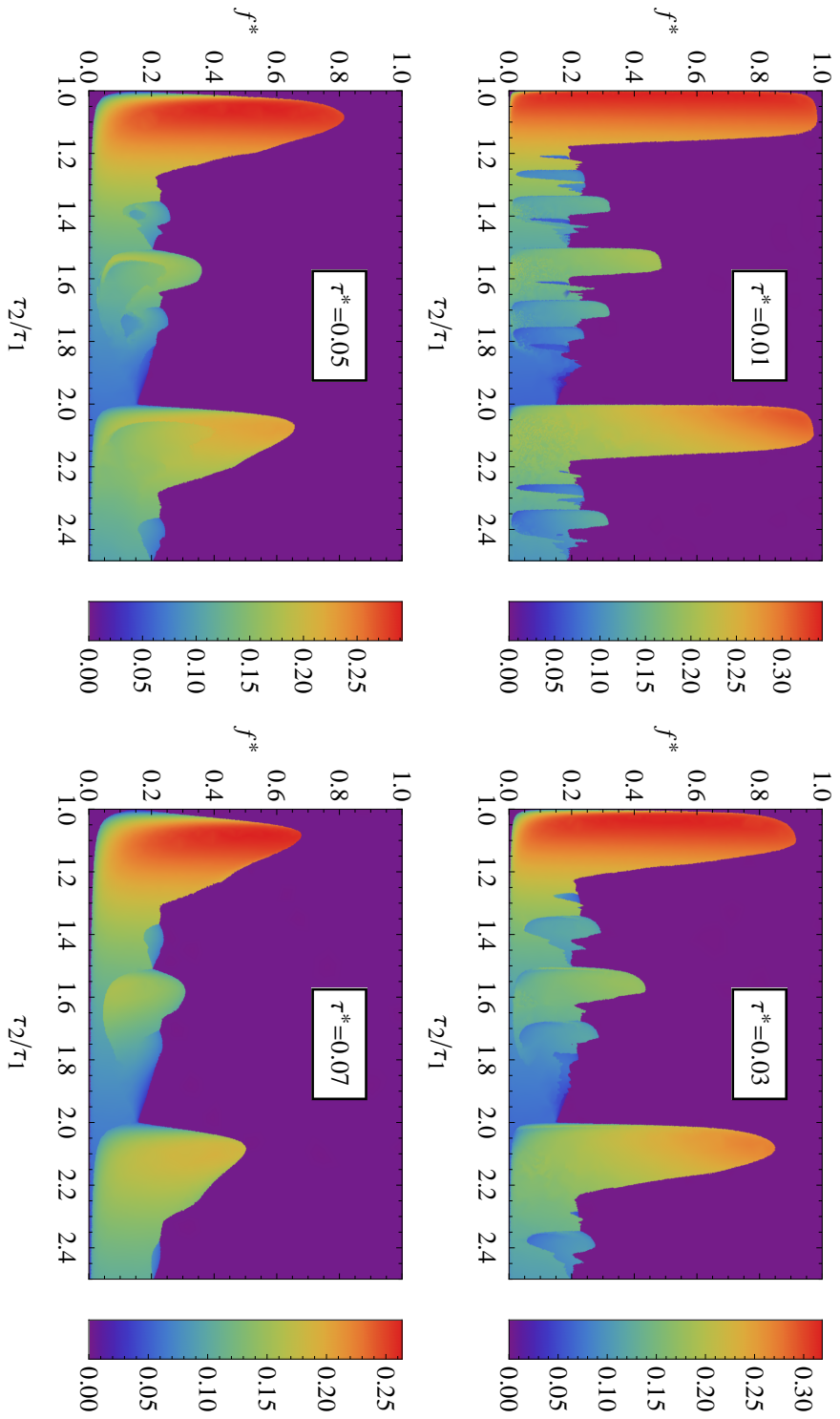


Figure 4.5: The phase space of model 1 for four different values of  $\tau^*$ : 0.01, 0.03, 0.05, 0.07. In all other simulations,  $\tau^* = 0.03$  was used. This is not representative of the  $\tau^* \rightarrow 0$  limit, as the structure of the phase space changes as  $\tau^*$  is decreased.

# Selected bibliography

- [1] Jayanth R. Banavar and Amos Maritan. Ecology: Towards a theory of biodiversity. *Nature*, 460(7253):334–5, 2009.
- [2] Richard Condit. *Tropical forest census plots: methods and results from Barro Colorado Island, Panama and a comparison with other plots*. Springer, 1998.
- [3] **Szabolcs Horvát**, Aranka Derzsi, Zoltán Nédá, and Adalbert Balog. A spatially explicit model for tropical tree diversity patterns. *Journal of Theoretical Biology*, 265(4):517–23, 2010.
- [4] **Szabolcs Horvát**, E Ágnes Horváth, Gabriell Máté, Erna Káptalan, and Zoltán Nédá. Unexpected synchronization. *Journal of Physics: Conference Series*, 182:012026, 2009.
- [5] **Szabolcs Horvát**, Volodymyr K. Magas, Daniel D. Strottman, and László P. Csernai. Entropy development in ideal relativistic fluid dynamics with the bag model equation of state. *Physics Letters B*, 692:277–280, 2010.
- [6] **Szabolcs Horvát** and Zoltán Nédá. Complex phase space of a simple synchronization model, 2012. submitted to the New Journal of Physics.
- [7] **Szabolcs Horvát** and Zoltán Nédá. Synchronization in a two-mode oscillator ensemble. In *37th Conference on the Middle European Cooperation in Statistical Physics*, 2012.
- [8] Stephen P. Hubbell. *The unified neutral theory of biodiversity and biogeography*. Princeton University Press, 2001.

- [9] Z. Néda, A. Nikitin, and T. Vicsek. Synchronization of two-mode stochastic oscillators: a new model for rhythmic applause and much more. *Physica A: Statistical Mechanics and its Applications*, 321(1-2):238–247, 2003.
- [10] Z. Néda, E. Ravasz, Y. Brechet, T. Vicsek, and Albert-László Barabási. The sound of many hands clapping. *Nature*, 403(6772):849–50, 2000.
- [11] Z. Néda, E. Ravasz, T. Vicsek, Y. Brechet, and A. L. Barabási. Physics of the rhythmic applause. *Physical Review E Statistical Physics Plasmas Fluids And Related Interdisciplinary Topics*, 61(6 Pt B):6987–6992, 2000.
- [12] A. Nikitin, Z. Néda, and T. Vicsek. Collective Dynamics of Two-Mode Stochastic Oscillators. *Physical Review Letters*, 87(2):2–5, 2001.
- [13] C. S. Peskin. Mathematical Aspects of Heart Physiology. In *Courant Institute of Mathematical Sciences*, pages 268–278. Courant Institute of Mathematical Sciences, 1975.
- [14] James Rosindell, Stephen P. Hubbell, and Rampal S. Etienne. The Unified Neutral Theory of Biodiversity and Biogeography at Age Ten. *Trends in ecology & evolution*, pages 1–9, 2011.
- [15] E. Sismondo. Synchronous, alternating, and phase-locked stridulation by a tropical katydid. *Science (New York, N. Y.)*, 249(4964):55–8, 1990.
- [16] K. Stern and M. K. McClintock. Regulation of ovulation by human pheromones. *Nature*, 392(6672):177–9, 1998.
- [17] R. Sumi, Z. Néda, a. Tunyagi, Sz. Boda, and Cs. Szász. Nontrivial spontaneous synchronization. *Physical Review E*, 79(5):1–9, 2009.
- [18] Igor Volkov, Jayanth R. Banavar, Stephen P. Hubbell, and Amos Maritan. Patterns of relative species abundance in rainforests and coral reefs. *Nature*, 450(7166):45–9, 2007.

- [19] Igor Volkov, Jayanth R. Banavar, Amos Maritan, and Stephen P. Hubbell. Neutral theory: the stability of forest biodiversity. *Nature*, 427(6976):696; discussion 696–7, 2004.
- [20] Tommaso Zillio, Igor Volkov, Jayanth R. Banavar, Stephen P. Hubbell, and Amos Maritan. Spatial Scaling in Model Plant Communities. *Physical Review Letters*, 95(9):1–4, 2005.



# Publications

## Publications related to the thesis

1. Sz. Horvát, Z. Nédá, *Complex phase space of a simple synchronization model*, manuscript submitted to the New Journal of Physics.  
<http://arxiv.org/abs/1203.1699>.
2. Sz. Horvát, A. Derzsi, Z. Nédá, and A. Balog, *A spatially explicit model for tropical tree diversity patterns*, **Journal of Theoretical Biology**, vol. **265**, no. 4, pp. 517-523, 2010.
3. Sz. Horvát, V. Magas, D. Strottman, and L. Csernai, *Entropy development in ideal relativistic fluid dynamics with the Bag Model equation of state*, **Physics Letters B**, vol. **692**, no. 4, pp. 277-280, 2010.
4. Sz. Horvát, E. Á. Horváth, G. Máté, E. Káptalan, Z. Nédá, *Unexpected synchronization*, **Journal of Physics: Conference Series**, vol. **182**, 012026, 2009

## Other publications

1. S. Zschocke, Sz. Horvát, I. Mishustin, L. P. Csernai, *Non-equilibrium hadronization and constituent quark number scaling*, **Physical Review C**, vol. **83**, p. 044903, 2011.
2. L. P. Csernai, Y. Cheng, Sz. Horvát, V. Magas, D. Strottman, and M. Zétényi, *Flow analysis with 3-dim ultra-relativistic hydro*, **Journal of Physics G**, vol. **36**, no. 6, p. 064032, 2009.

3. Sz. Horvát and P. Hantz, *Pattern formation induced by ion-selective surfaces: models and simulations*, **The Journal of Chemical Physics**, **123**, 34707, 2005
4. P. Hantz, J. Partridge, Gy. Láng, Sz. Horvát and M. Ujvári *Ion-Selective Membranes Involved in Pattern-Forming Processes*, **The Journal of Physical Chemistry B**, **108**, 18135-18139, 2004